J|A|C|S
COMMUNICATIONS

Published on Web 01/08/2002

Atomic Properties of N_2O_4 Based on Its Experimental Charge Density

Marc Messerschmidt,[†] Armin Wagner,[†] Ming Wah Wong,[‡] and Peter Luger*,[†]

Institute for Chemistry/Crystallography, Free University Berlin, Takustrasse 6, 14195 Berlin, Germany, and Department of Chemistry, National University of Singapore, Kent Ridge, Singapore 119260

Received July 24, 2001

Bader's theory of atoms in molecules (AIM)[1] provides a well-defined procedure of partitioning a molecule into atomic regions with zero-flux surfaces (ZFS) as boundaries. Surfaces of this type establish atomic basins around nuclear attractors of the corresponding trajectories of the electron density gradient vector field. As a result, each basin uniquely defines an atomic volume. With the knowledge of the shape and volume of an atom, a number of atomic or functional group properties can be evaluated; for instance, atomic charges can be obtained by integration over the charge density in the given atomic volume. Because of the nontrivial shape of the ZFS, they are not easy to evaluate. Although this procedure has been applied successfully to charge density analysis in theoretical calculations,[2] partitioning of experimental charge densities is only possible very recently, for example with the newly developed TOPXD program by Coppens et al.[3]Because the algorithm to derive the experimental ZFS is still very time-consuming, present applications are restricted to smaller molecules. Nitrogen dioxide is therefore considered as an ideal system for experimental investigation. Furthermore, the electronic structure and bonding of this species are of fundamental chemical interest. $NO_2^{\bullet}$ radical is known to exist in the crystal as a dimer N_2O_4, formed via addition of two $NO_2^{\bullet}$ radicals. N_2O_4 is characterized by a very long N−N bond length of 1.76 Å.[4] Nitrogen dioxide (mp = −15 °C) is a liquid at ambient conditions. In the present experiment, it was crystallized from the melt in an X-ray capillary at low-temperature conditions directly on the diffractometer. The cubic phase of N_2O_4 crystallizes in the space group $Im\bar{3}$. Due to the high Laue symmetry, a data set of high redundancy (average ≈ 17.8) could be collected.[5] After merging, a data set of 720 unique reflections ($\sin(\theta_{max}/\lambda) = 1.249$ Å^{-1}) was used for a multipole refinement according to the Hansen−Coppens formalism[6] up to the hexadecapole level with the XD program.[7] The refinement led to a reasonable fit ($R(F) = 2.17\%$) with a maximum residual density of 0.14 e/Å^3. From the obtained multipole parameters,[8] a topological analysis of charge density was performed and atomic properties were evaluated.

N_2O_4, a prototypical species of weakly bonded systems, has been the subject also of intense theoretical interest.[9−11] A comprehensive theoretical study by Schaefer et al. has shown that this weakly bonded system can be described properly by using single reference treatments.[9] In addition, Kovacs et al. have indicated that DFT calculations can reproduce well the structure and vibrational spectra of N_2O_4.[10] Here, we have employed the B3LYP functional in conjunction with the 6-31G(d) basis set to investigate the structure and charge density of N_2O_4[12] and to compare with the experimental findings. We note that the calculated N−N and N−O bond lengths are in excellent agreement with experiment (Table 1). To gain further insight into the electronic structure of this intriguing species,

Table 1. Electron Densities at BCPs[a]

bond	d [Å]	ρ_b [e/Å^3]	$\nabla^2\rho_b$ [e/Å^5]	ϵ
N−O	1.1902(3)	3.69(3)	−27.30(13)	0.10
	1.196	3.63	−26.60	0.07
N−N	1.7586(7)	1.22(1)	0.83(3)	0.19
	1.781	1.00	1.83	0.13

[a] Theoretical values in second row.

Table 2. N-N BCP's of Model Compounds

compound	n	HF/6-31G(d) ρ_b [e/Å^3]	B3LYP/6-31G(d) ρ_b [e/Å^3]
N_2H_4	1	2.20	2.04
N_2H_2	2	3.48	3.21
N_2	3	4.80	4.48

the AIM[1] topological analysis was carried out using the Morphy98[13] and TOPXD[3] programs. A summary of experimental and theoretical topological descriptors at the bond critical points (BCPs defined by the condition that $\nabla\rho_b$ vanishes) of N_2O_4 is given in Table 1.

The bond strength (or bond order) of N_2O_4 is of chemical interest because of the extremely long N−N bond length of 1.76 Å. To obtain quantitative information about the bond order (n), the value of charge density ρ_b at the BCP of a model set of N−N and N−O containing compounds, namely N_2H_4, N_2H_2, N_2, H_3NO, HNO_3, HNO_2, HNO, N_2O_2 were considered. Since experimental charge densities of these compounds are not available, the B3LYP/6-31G-(d) wave functions were used for this purpose. From the calculations, N−O single and double bonds correspond to ρ_b value of 2.48(32) e/Å^3 and 3.60(20) e/Å^3, respectively. Thus, the N−O bonds in N_2O_4 are equivalent to that of a normal double bond. If a linear fit is applied to the bond order/ theoretical $\rho_b$value distribution (Table 2) an estimate bond order of $n \approx 0.5$ is obtained for the N−N bond in N_2O_4. However, an extrapolation to bond orders smaller than one is uncertain. For the relation between bond order and ρ_b values Bader[1] suggests an exponential function for C−C bonds and recommends a linear fit for N−N bonds. In both cases the extrapolation to zero bond order is not well defined. The rather weak N−N bond may be attributed to the strong repulsion between the oxygen lone pairs and the strong positively charged nitrogen atoms.

The valence-shell charge concentrations (VSCCs) are illustrated by the experimental Laplacian representation in Figure 1. The positions of the VSCCs at the oxygen are somewhat surprising because they are orthogonal to the N−O bond and form an angle of 174/156° (experiment/theory) with the oxygen atom. These positions can be explained with the sp-hybridized oxygen, which is in agreement with the theoretically calculated molecular orbitals (MOs). Inspection of the MOs indicates that there are orthogonal π-systems that form the N−O bond in addition to σ bonding MOs. Thus, in this case the localized VSCCs on oxygen are involved in the π bonds and do not correspond to lone pairs of the oxygen.

An atomic partitioning making use of the ZFS was performed

* Author for correspondence. Fax: +49(30)838-53464. E-mail: luger@chemie.fu-berlin.de.
[†] Free University Berlin.
[‡] National University of Singapore.

10.1021/ja011802c CCC: $22.00

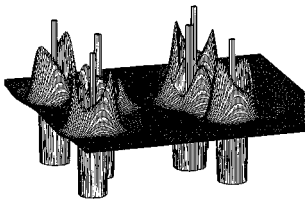

Figure 1. Experimental Laplacian distribution.

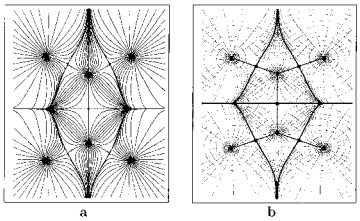

Figure 2. Experimental (a) and theoretical (b) gradient vector field.

Table 3. Atomic Volumes in Å^3 [a]

	expt	B3LYP/6-31G(d)	B3LYP/6-311+G(d)	B3LYP/6-311+(3df)
N	7.9	7.4	7.7	7.3
O	15.5	16.5	16.9	17.2

[a] Theoretical volumes were obtained from electron density contour of $\rho = 0.001$ au.

with TOPXD.[3] As illustrated by the gradient vector field (Figure 2), the shape and atomic volumes derived by experiment and theory (Table 3) are very similar. The cutoff $\rho = 0.001$ au, which is normally used in theory,[14] seems justified by the TOPXD findings in that its application to the experiment gives 98% of the ZFS atomic volumes. The atomic volume of oxygen is about twice that of nitrogen, and the sum multiplied by the number of atoms in the unit cell reproduces within less than 0.1% the cell volume obtained from X-ray experiment.

Finally, we examine the atomic charges derived from experiment and theory. Atomic charge is an important property, which is often used to rationalize structural and reactivity differences. Numerous definitions of atomic charges and atomic populations have been published in the literature.[15] Thus, it is instructive to provide a detailed comparison. The experimental atomic populations were obtained by integrating the charge density contributions over the atomic regions defined by the zero-flux surfaces, and the experimentally derived charges for N and O atoms are 0.464 and −0.235, respectively. For calculated atomic populations, we have considered four commonly used methods of computing atomic charges: (1) Mulliken,[16] (2) AIM,[1] (3) natural population (NPA),[17] and (4) the CHELP[18] analysis. The Mulliken and NPA methods are partition schemes based on the basis functions that are used to represent the wave functions, while CHELP charges are derived by fitting the electrostatic potential. The calculated charges using the Hartree−Fock (HF), B3LYP, and MP2 methods, based on the crystal geometry, are summarized in Table 4. Three different basis sets, namely 6-31G(d), 6-31+G(d), and 6-311+G(3df), were employed. Not surprisingly, the Mulliken charges are strongly basis-set dependent. Peculiarly, calculations with the 6-311+G(d) basis set predict the wrong sign in atomic charges. The calculated charges for the other three methods are less basis-set dependent. The AIM charges are rather independent of the theoretical method used. However, they are consistently too high compared to the experimental values. Few studies of experimental and theoretical AIM charges exist. Hence, it is uncertain, how the crystal field may influence the charge distribution. Additional periodic HF and B3LYP calculations[19] support the nonperiodic results (Table 4). The multipole model, which fits the experimental data, is based on Slater type functions and has been reported to be of insufficient flexibility.[20] Thus, the influence of the model on the AIM charges has to be further examined.

Table 4. Calculated Atomic Charges Based on Experimental Geometry

	Mulliken		AIM		NPA		CHELP	
level	N	O	N	O	N	O	N	O
HF/6-31G(d)	0.71	−0.35	0.81	−0.41	0.71	−0.35	0.63	−0.31
HF/6-311+G(d)	0.00	0.00	0.81	−0.41	0.69	−0.35	0.66	−0.33
HF/6-311+G(3df)	0.96	−0.48	0.86	−0.43	0.71	−0.35	0.61	−0.30
B3LYP/6-31G(d)	0.60	−0.30	0.73	−0.37	0.55	−0.27	0.51	−0.25
B3LYP/6-311+G(d)	−0.10	0.05	0.72	−0.36	0.54	−0.27	0.56	−0.28
B3LYP/6-311+G(3df)	0.65	−0.33	0.76	−0.38	0.55	−0.27	0.53	−0.26
MP2/6-31G(d)	0.52	−0.26	0.73	−0.37	0.50	−0.25	0.48	−0.24
MP2/6-311+G(d)	−0.15	0.07	0.73	−0.37	0.48	−0.24	0.52	−0.26
MP2/6-311+G(3df)	0.75	−0.38	0.77	−0.39	0.49	−0.25	0.48	−0.24
PHF/6-21G(d)			0.94	−0.47				
PB3LYP/6-21G(d)			0.83	−0.41				
experiment			0.46	−0.24				

Both NPA and CHELP procedures give more comparable atomic charges. Their HF values are somewhat too high, but inclusion of electron correlation lowers the computed charges appreciably. At both B3LYP and MP2 levels, the calculated charges are close to the experimental derived values. It is important to note also that the observed trend in atomic charges is independent of the geometry used (see Supporting Information). Further work is in progress to examine whether our findings are of general nature.

Supporting Information Available: Additional tables (PDF). This material is available free of charge via the Internet at http://pubs.acs.org.

References

(1) Bader, R. F. W. *Atoms in Molecules*; Clarendon Press: Oxford, 1994.
(2) Biegler-König, F. W.; Bader, R. F. W.; Tang, T.-H. *J. Comp. Chem.* **1982**, *3*, 317.
(3) Volkov, A.; Gatti, C.; Abramov, Yu.; Coppens, P. *Acta Crystallogr., Sect. A* **2000**, *56*, 252.
(4) Kvick, Å.; McMullan, R. K.; Newton, M. D. *J. Chem. Phys.* **1982**, *76*, 3754.
(5) Crystal data collected with Bruker Smart 1000: $a = 7.764(1)$ Å, cubic, space group *Im3*, $Z = 6$, 16918 reflections (712 unique, $R_{int} = 2.83\%$) were collected at $T = 100$ K, $\lambda = 0.71073$ Å ($\sin(\theta_{max}/\lambda) = 1.249$ Å^{-1}).
(6) Hansen, N. K.; Coppens, P. *Acta Crystallogr.* **1978**, *A34*, 909.
(7) Koritsánszky, T.; Howard, S.; Mallinson, R. P., Su, Z.; Richter, T.; Hansen, N. K. XD, A Computer Program Package for Multipole Refinement and Analysis of Charge Densities from X-ray Diffraction Data, 1995.
(8) For further details of the multipole refinement, see: Supporting Information.
(9) Weslowski, S. S.; Fermann, J. T.; Crawford, T. D.; Schaefer, H. F., *J. Chem. Phys.* **1997**, *106*, 7178.
(10) Kovacs, A.; Borisenko, K. B.; Pongor, G, *Chem. Phys. Lett.* **1997**, *280*, 451.
(11) Jursic, B. S. *Int. J. Quant. Chem.* **1996**, *58*, 41.
(12) Calculations were performed using the Gaussian 98 programs: Frisch, M. J.; Trucks, G. W.; Schlegel, H. B.; Scuseria, G. E.; Robb, M. A.; Cheeseman, J. R.; Zakrzewski, V. G.; Montgomery, J. A., Jr.; Stratmann, R. E.; Burant, J. C.; Dapprich, S.; Millam, J. M.; Daniels, A. D.; Kudin, K. N.; Strain, M. C.; Farkas, O.; Tomasi, J.; Barone, V.; Cossi, M.; Cammi, R.; Mennucci, B.; Pomelli, C.; Adamo, C.; Clifford, S.; Ochterski, J.; Petersson, G. A.; Ayala, P. Y.; Cui, Q.; Morokuma, K.; Malick, D. K.; Rabuck, A. D.; Raghavachari, K.; Foresman, J. B.; Cioslowski, J.; Ortiz, J. V.; Stefanov, B. B.; Liu, G.; Liashenko, A.; Piskorz, P.; Komaromi, I.; Gomperts, R.; Martin, R. L.; Fox, D. J.; Keith, T.; Al-Laham, M. A.; Peng, C. Y.; Nanayakkara, A.; Gonzalez, C.; Challacombe, M.; Gill, P. M. W.; Johnson, B. G.; Chen, W.; Wong, M. W.; Andres, J. L.; Head-Gordon, M.; Replogle, E. S.; Pople, J. A. *Gaussian 98*, revision A.7; Gaussian, Inc.: Pittsburgh, PA, 1998.
(13) MORPHY98, a program written by P. L. A. Popelier with a contribution from R. G. A. Bone, UMIST, Manchester, England, EU, 1998.
(14) Bader, R. F. W.; Carroll, T.; Cheeseman, J. R.; Chang, C., *J. Am. Chem. Soc.* **1987**, *109*, 7968.
(15) For leading references, see: Wiberg, K. B.; Rablen, P. R., *J. Comput. Chem.* **1993**, *14*, 1504.
(16) Mulliken, R. S. *J. Chem. Phys.* **1962**, *36*, 3428.
(17) Reed, A. E.; Curtiss, L. A.; Weinhold, F. *Chem. Rev.* **1988**, *88*, 899.
(18) Chirlin, L. E.; Francl, M. M. *J. Comp. Chem.* **1987**, *8*, 894.
(19) Saunders,V. R.; Dovesi, R.; Roetti, C.; Causá, M; Harrison, N. M.; Orlando, R.; Zicovich-Wilson, C. M., Crystal98 User's Manual, University of Torino, Torino, 1998.
(20) Volkov, A.; Abramov, Yu.; Coppens, P.; Gatti C. *Acta Crystallogr. Sect. A* **2000**, *56*, 332.

JA011802C